Isopropylcyclopropane + OH Gas Phase Reaction: A Quantum Chemistry + CVT/SCT Approach

Annia Galano,*,† Armando Cruz-Torres,† and J. Raúl Alvarez-Idaboy*,‡

Instituto Mexicano del Petróleo, Eje Central Lázaro Cárdenas 152, 07730 México D. F., México, and Facultad de Química, Universidad Nacional Autónoma de México, Ciudad Universitaria, 04510 México D. F., México

Received: October 25, 2005; In Final Form: December 12, 2005

A theoretical study of the mechanism and kinetics of the OH hydrogen abstraction from isopropylcyclopropane (IPCP) is presented. Optimum geometries, frequencies and gradients have been computed at the BHandHLYP/6-311++G(d,p) level of theory for all stationary points, as well as for additional points along the minimum energy path (MEP). Energies have been improved by single-point calculations at the above geometries using CCSD(T)/6-311++G(d,p) to produce the potential energy surface. The rate coefficients are calculated for the temperature range 260−350 K by using canonical variational theory (CVT) with small-curvature tunneling (SCT) corrections. Our analysis suggests a stepwise mechanism involving the formation of a reactant complex in the entrance channel and a product complex in the exit channel, for all the modeled paths. The reactant complexes are examined in detail, because they exhibit *alkene-like* structure. The excellent agreement between the overall calculated and experimental rate coefficients at 298 K supports the reliability of the parameters obtained for the temperature dependence and branching ratios of the IPCP + OH reaction, proposed here for the fist time. The expression that best describes the studied reaction is $k_{overall} = 6.15 \times 10^{-13} e^{1747/RT}$ $cm^3 \cdot molecule^{-1} \cdot s^{-1}$. The predicted activation energy is −0.89 kcal/mol.

Introduction

The gas phase reactions of OH radicals with volatile organic compounds (VOCs) have become of great interest due to their relevance to the tropospheric chemistry. These reactions have been widely studied for alkanes as well as for cyclopropane. However, there is very limited information on alkyl-substituted cyclopropanes.[1,2] In addition, the reactions of this kind of compounds are interesting themselves, due to the chemical peculiarities of the small rings. These are susceptible to undergo addition reactions yielding open-chain products, in addition to the abstraction reactions that are characteristic of cycloalkanes and alkanes.

The only study of the isopropylcyclopropane (C_6H_{12}) + OH reaction to date is that of Atkinson and Aschmann.[1] They reported a rate coefficient of 2.83×10^{-12} $cm^3 \cdot molecule^{-1} \cdot s^{-1}$ and studied the influence of the cycle on the structure−activity relationships (SAR).[3−6] However, there are no data available on the temperature dependence of the rate coefficient or on the branching ratios for this reaction.

Thus, the aim of this work is to determine Arrhenius parameters for the OH radical reaction with isopropylcyclopropane (IPCP), as well as to study the different channels of reaction and their contribution to the overall rate coefficient. These data are reported here for the first time and might be useful in air quality models. Additionally, *alkene-like* reactant complexes were found in the course of the modeling of the reaction paths, and they have been studied in detail.

Computational Details

Five reaction channels have been computed, four of them corresponding to hydrogen abstraction channels (I−IV, Figure 1) and an additional one (V) corresponding to the addition of the OH radical to one of the carbon atoms in the ring. The abstraction paths have been modeled according to a three-step mechanism, namely, (1) the formation of the reactant complex from the isolated reactants, (2) the formation of the product complex from the reactant complex, and (3) the formation of the corresponding radical and water from the product complex:

$$\mathrm{IPCP} + {}^{\bullet}\mathrm{OH} \underset{k_{-1}}{\overset{k_1}{\rightleftharpoons}} [\mathrm{RC}]^{\bullet} \xrightarrow{k_2} [\mathrm{PC}]^{\bullet} \underset{k_{-3}}{\overset{k_3}{\rightleftharpoons}} \mathrm{R}^{\bullet} + \mathrm{H_2O} \quad \text{(I-IV)}$$

where IPCP represents isopropylcyclopropane, and RC, PC and R represent the reactant complex, product complex and radical product corresponding to each particular path.

The addition channel was modeled as a two steps mechanism:

$$\mathrm{IPCP} + {}^{\bullet}\mathrm{OH} \underset{k_{-1}}{\overset{k_1}{\rightleftharpoons}} [\mathrm{RC}]^{\bullet} \xrightarrow{k_2} [\mathrm{C_6H_{12}{-}OH}]^{\bullet} \quad \text{(V)}$$

Full geometry optimizations of all the stationary points were performed with the Gaussian 98[7] program using the BHandHLYP hybrid HF-density functional[8,9] and the 6-311++G(d,p) basis set. The energies of all the stationary points were improved by single point calculations at the CCSD(T)/6-311++G(d,p) level of theory. Unrestricted calculations were used for open shell systems. Frequency calculations were carried out for all the stationary points at the DFT level of theory and local minima and transition states were identified by the number of imaginary frequencies (NIMAG = 0 or 1, respectively). Zero point energies (ZPE) and thermal corrections to the energy (TCE) at 298.15 K were included in the determination of the activation energies and of the heats of reaction, respectively.

Rate coefficients were calculated using the canonical variational theory (CVT)[10−16] and small-curvature tunneling (SCT)[13−19] corrections, implemented in the www.cseo.net web site.[20] The

* Corresponding authors. E-mail: A.G., agalano@imp.mx; J.R.A.-I., jidaboy@servidor.unam.mx.
† Instituto Mexicano del Petróleo.
‡ Universidad Nacional Autónoma de México.

10.1021/jp056117x CCC: $33.50 © 2006 American Chemical Society
Published on Web 01/13/2006

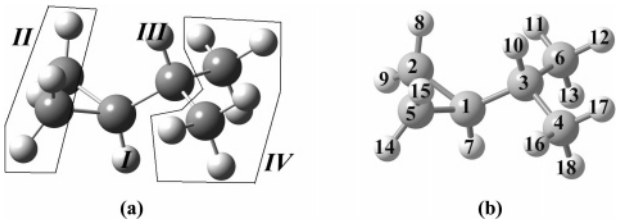

Figure 1. (a) Hydrogen atoms to be abstracted in each abstraction channel. (b) Atom numbering.

minimum-energy paths (MEP)[21,22] were calculated by the intrinsic reaction coordinate (IRC) method[23,24] at the BHandHLYP/6-311G++(d,p) level of theory. The MEP was calculated in mass-scaled Cartesian coordinates.[25,26] Two hundred points were modeled on either side of the saddle points, with a gradient step size of 0.01 bohr. Force constants, harmonic vibrational frequencies and normal-mode vectors for the $3N - 7$ degrees of freedom that are orthogonal to the reaction path were computed at selected points along the IRC.

The canonical variational theory (CVT)[10−16] is an extension of the transition state theory (TST).[27,28] This theory minimizes the errors due to recrossing trajectories[29−31] by moving the dividing surface along the MEP so as to minimize the rate. The reaction coordinate (s) is defined as the distance along the MEP, with the origin located at the saddle point and is negative on the reactants side and positive on the products side of the MEP. For a canonical ensemble at a given temperature T, the canonical variational theory (CVT) thermal rate constant is given by

$$k^{\mathrm{CVT}}(T,s) = \min\{k^{\mathrm{GT}}(T,s)\} \qquad (1)$$

where $k^{\mathrm{GT}}(T,s)$ is the rate constant for the passage through the generalized transition state (GT)[32−36] that intersects the MEP at s:

$$k^{\mathrm{GT}}(T,s) = \sigma(s)\frac{k_{\mathrm{B}}T}{h}\frac{Q^{\mathrm{GT}}(T,s)}{Q^{\mathrm{R}}(T)}\exp\left[-\frac{V_{\mathrm{MEP}}(s)}{k_{\mathrm{B}}T}\right] \qquad (2)$$

In this expression, $\sigma(s)$ is the reaction path symmetry factor, k_{B} and h are the Boltzmann and Planck constants, T is temperature, Q^{GT} and Q^{R} are the partition functions of the generalized transition state and of the reactants, and $V_{\mathrm{MEP}}(s)$ is the potential energy of the MEP at s.

Because accurate rate constant calculations require the proper computation of the partition functions (Q), the hindered rotor approximation has been used to correct the Q's corresponding to internal rotations with torsional barriers comparable to RT. The modes corresponding to hindered rotations were identified by direct inspection from frequency calculations and using the GaussView tool. Then, these modes were removed from the vibrational partition function of the corresponding speciesand replaced with the hindered rotor partition function (Q^{HR}). In our calculations we have adopted the analytical approximation to Q^{HR} for a one-dimensional hindered internal rotation proposed by Ayala and Schlegel.[37]

The quantum mechanical effect on the motion along the reaction coordinate is included in the kinetics calculations by multiplying the CVT rate constant by a temperature-dependent transmission coefficient $\kappa(T)$. Therefore, the final expression for the rate constant is given by

$$k(T) = \kappa(T)k^{\mathrm{CVT}}(T,s) \qquad (3)$$

where $k(T)$ can be computed using the small-curvature (SCT) method,[13−19] which constitutes a generalization of the Marcus−Coltrin method.[38] In SCT it is assumed that the tunneling path is displaced from the MEP to a concave-side vibrational turning point in the direction of the internal centrifugal force. In this method, the probability that a system with energy E be transmitted through the ground-state level of the transition state is approximated by the centrifugal-dominant small-curvature semiclassical adiabatic ground-state method (CD-SCSAG).[39,40] The SCT transmission coefficient includes the effect of the reaction path curvature on the transmission probability, $P(E)$, which is calculated as

$$P(E) = 1/\{1 + \exp[2\theta(E)]\} \qquad (4)$$

where $\theta(E)$ is the imaginary action integral evaluated along the tunneling path:

$$\theta(E) = \frac{2\pi}{h}\int_{S1}^{S2}\sqrt{2\mu_{\mathrm{eff}}(s)|E - V_{\mathrm{a}}^{G}(s)|}\,\mathrm{d}s \qquad (5)$$

The integration limits S_1 and S_2 are the reaction coordinate classical turning points; μ_{eff} is the reduced mass, which introduces the reaction path curvature; and $V_{\mathrm{a}}^{G}(s)$ is the adiabatic ground-state potential.

Results and Discussion

Geometries. Reactant and product complexes were obtained from the IRC calculations, by minimization of the corresponding ends. In all, four reactant complexes were identified, because all the hydrogen atoms in the cluster labeled as II (Figure 1) will react the same way, and so will all of the hydrogen atoms in the cluster labeled as IV. The presence of this kind of adduct is quite unexpected due to the IPCP lack of polar groups. The main interaction leading to the complexes formation seems to occur between the H atom in the OH radical and the C−C bonds in the cyclopropyl ring. This interaction is similar to that found in alkenes + OH reactions.[41] The high p character of the C−C bonds in cyclopropane and its tendency to show alkene-like behavior have been previously reported.[42−49] However, to the best of our knowledge, the existence of the *alkene-like* complexes reported in here, has not been formerly described.

To determine the extra p contribution to the ring bonds in IPCP, natural bond orbital (NBO) analyses[50−54] were performed using the NBO 3.1 program,[55] as implemented in the Gaussian 98 package. The NBO for a localized σ bond between atoms A and B (σ_{AB}) is formed from directed orthonormal hybrids h_{A}, h_{B} (natural hybrid orbitals, NHOs)

$$\sigma_{\mathrm{AB}} = c_{\mathrm{A}}h_{\mathrm{A}} + c_{\mathrm{B}}h_{\mathrm{B}}$$

and the natural hybrids in turn are composed from a set of effective valence-shell atomic orbitals (natural atomic orbitals, NAOs), optimized for the chosen wave function. In the orbital hybridization, as originally formulated by Pauling[56] and Slater,[57] the sp^n hybrids of a central atom depend only on the number of ligands to be bonded, but for inequivalent ligands or unequal bond angles it is necessary to consider more general sp^{λ}, where λ is generally noninteger (for more details see ref 50 and references there in). The NBO analysis of the IPCP wave function led to the following σ_{CC} orbitals for the ring fragment:

$$\sigma_{C_1C_2} = 0.7086(sp^{3.61})_{C_1} + 0.7057(sp^{3.26})_{C_2}$$

$$\sigma_{C_1C_5} = 0.7086(sp^{3.61})_{C_1} + 0.7057(sp^{3.26})_{C_5}$$

$$\sigma_{C_2C_5} = 0.7071(sp^{3.57})_{C_2} + 0.7071(sp^{3.57})_{C_5}$$

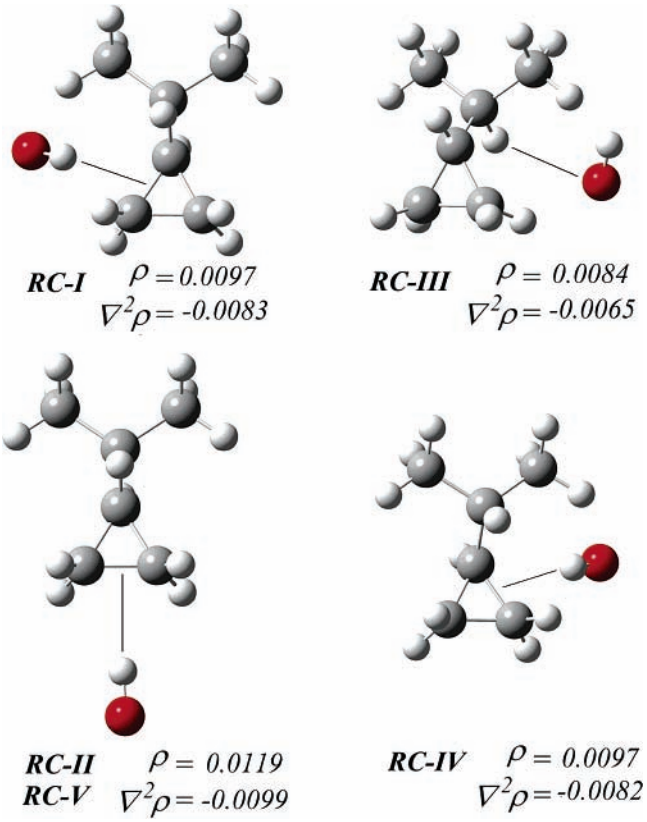

Figure 2. Fully optimized BHandHLYP/6-311++G(d,p) reactant complexes of the IPCP + OH reaction.

TABLE 1: Deviation Angles of NHOs (Dev, in Degrees) from the Line of Nuclear Centers ($\alpha \cong \beta$)

NHO	IPCP	RC−I	RC−II	RC−III	RC−IV
$h_{C_1}(\sigma_{C_1C_2})$	22.3	**24.0**	21.8	23.2	22.7
$h_{C_2}(\sigma_{C_1C_2})$	23.4	**24.4**	23.1	23.5	23.1
$h_{C_1}(\sigma_{C_1C_5})$	22.3	22.7	21.8	23.1	**24.0**
$h_{C_5}(\sigma_{C_1C_5})$	23.4	23.1	23.0	23.3	**24.4**
$h_{C_2}(\sigma_{C_2C_5})$	23.4	23.1	**24.5**	23.4	23.1
$h_{C_5}(\sigma_{C_2C_5})$	23.4	23.1	**24.6**	23.4	23.1

According to these results there is an "extra" p character ($\lambda > 3$) in the C−C bonds of the isopropyl ring, which seems to justify the alkene-like interactions found in the reactant complexes.

NBO analysis also yields information about the direction of the natural hybrid orbitals. Deviations from the line of nuclear centers are used to show the changes of directions of natural hybrid orbitals, i.e., the *bond bendings*. Because the bonds in cyclopropane rings are often described as *banana-like*, we consider it of interest to report here such bond bendings as the deviation angle (in degrees) between these two directions in IPCP, and in the reactant complexes (RC) formed through interaction of the OH radical with the cyclopropyl ring (Table 1, geometries in Figure 2). The deviation values corresponding to the bonds involved in the complexes formation have been highlighted (bold), and it can be noticed that their bending increases toward the interaction with the OH radicals, as it should be expected.

To confirm the interactions leading to the reactant complexes formation, Bader topological analysis[58] of the BHandHLYP/6-311G(d,p) wave functions were also performed and several critical points were found. The electronic charge density (ρ) and the Laplacian of $\rho(\nabla^2)$ corresponding to the main interaction in each reactant complex are reported in Figure 2. Two attractive

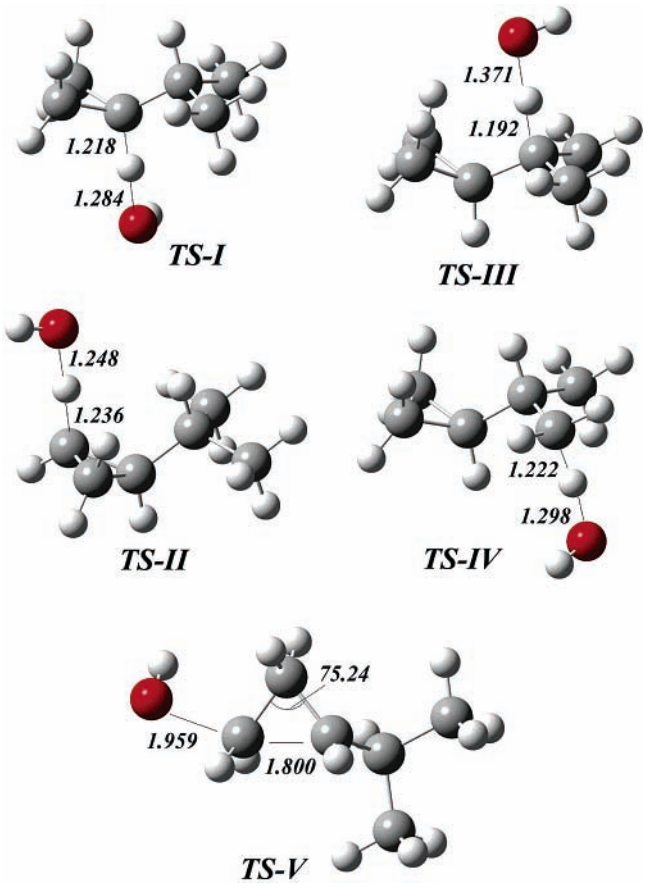

Figure 3. Fully optimized BHandHLYP/6-311++G(d,p) transition states of the IPCP + OH reaction.

interactions are responsible for the formation of the reactant complex corresponding to the abstraction from the −CH< group in the ring (RC−I). The main one is that shown in Figure 2, with distances $d(H_{OH}-C_1)$ and $d(H_{OH}-C_2)$ equal to 2.60 and 2.47 Å, respectively (see Figure 1b for atoms numbering). A weaker interaction was found between the O in the OH radical and one of the H the methyl groups, with $d(O_{OH}-H_{11})$ equal to 2.98 Å, $\rho = 0.0053$ and $\nabla^2\rho = -0.0049$. RC−II, which also corresponds to the addition path (V) is caused by only one interaction, with $d(H_{OH}-C_2)$ and $d(H_{OH}-C_5)$ equal to 2.40 and 2.43 Å, respectively. This is the adduct which resembles the most the alkenesLOH complexes. The reactant complex corresponding to the abstraction from the −CH< in the isopropyl group (RC−III) was found to be formed through three interactions, none of them alkene-like. The corresponding distances are $d(O_{OH}-H_{10}) = 2.59$ Å, $d(O_{OH}-H_8) = 3.02$ Å, and $d(O_{OH}-H_{11}) = 3.07$ Å, being the $O_{OH}\cdots H_{10}$ the strongest one (Figure 2). For the other two, the Bader analysis led to $\rho(O_{OH}-H_8) = 0.0063$, $\rho(\nabla^2)(O_{OH}-H_8) = -0.0058$, $\rho(O_{OH}-H_{11}) = 0.0029$, and $\rho(\nabla^2)(O_{OH}-H_{11}) = -0.0026$. Two attractive interactions contribute to RC−IV formation, the main one is alkene-like with $d(H_{OH}-C_1)$ and $d(H_{OH}-C_5)$ equal to 2.61 and 2.47 Å, respectively. The other occurs between the O in the OH radical and H16, with $d(O_{OH}-H_{16}) = 2.98$ Å, $\rho = 0.0052$ and $\nabla^2\rho = -0.0048$.

All the transition state (TS) structures considered in this work are shown in Figure 3. The main structural change associated with the formation of TS−I is an elongation of $d(C_1-H_7)$ by 0.138 Å, compared to free isopropylcyclopropane. Other minor variations observed in TS−I with respect to free reactants are the shortening of the C1C2 and C1C5 bonds by 0.013 Å. The

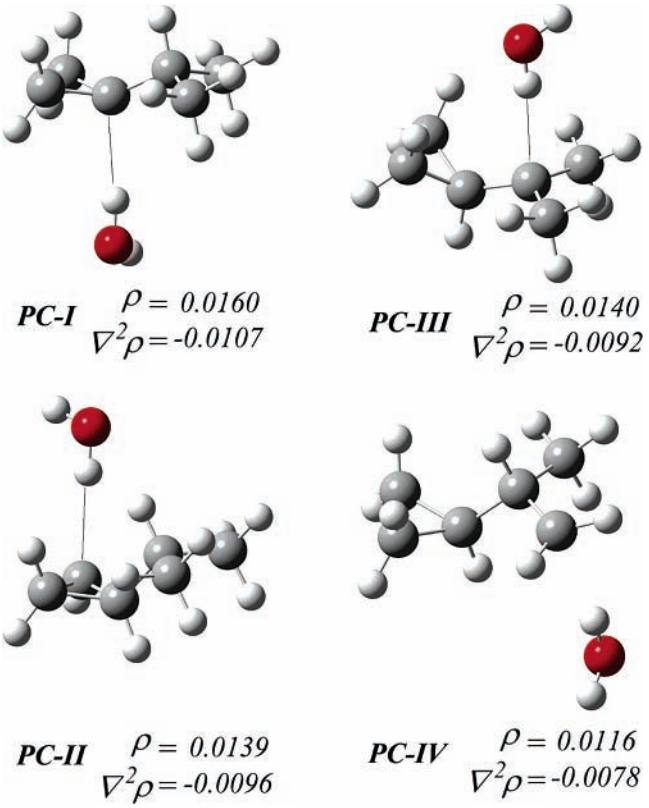

Figure 4. Fully optimized BHandHLYP/6-311++G(d,p) product complexes of the IPCP + OH reaction.

attack of the OH radical is found to be almost collinear, with the OH7C1 angle equal to 173.9°. TS−II in Figure 2 corresponds to abstraction from the $-CH_2-$ groups in the ring. It shows an elongation of 0.159 Å compared to the free reactant, and slight shortening of distances C1−C2 and C2−C5, by 0.013 and 0.017, respectively. The OH attack shows a OH8C2 angle of 173.3°. The transition state corresponding to channel III shows an elongation of 0.101 Å of the C3H10 bond, and shortenings of 0.010 Å in the C3C4 and C3C6 bonds. TSV shows a 0.304 Å elongation of the C1C2 bond and a C1C5C2 angle increased by 15° with respect to IPCP. It also shows a small shortening of d(C2−C5) by 0.011 Å.

Four product complexes (PC) corresponding to all the abstraction paths have been also modeled and fully optimized. Bader topological analysis of their BHandHLYP/6-311++G(d,p) wave functions were performed and the corresponding bond critical point were found. The values of ρ and $\nabla^2\rho$ are reported in Figure 4. The PCs are formed through attractive interactions between an H in the water molecule and the C atom in the IPCP radical, where the abstracted hydrogens were originally attached. The interaction distance were found to be $d(H_{H_2O}-C_1) = 2.234$ Å, $d(H_{H_2O}-C_2) = 2.288$ Å, $d(H_{H_2O}-C_3) = 2.307$ Å, and $d(H_{H_2O}-C_4) = 2.372$ Å, for PC−I, PC−II, PC−III and PC−IV, respectively.

The four abstractions products and the addition (open-ring) product were also fully optimized. However, for the sake of shortness, the discussion of their geometries has not been included in this manuscript.

Energies. The energies of all the modeled stationary points, relative to the isolated reactants, are shown in Table 2. They show that all the studied stationary points are lower in energy than the isolated reactants, with the exception of the transition

TABLE 2: CCSD(T)//BHandHLYP/6-311++G(d,p) Energies, in kcal/mol, Relative to the Isolated Reactants

channel	RC[a]	TS[a]	PC[b]	prod.[b]
I	−4.80	−1.98	−14.49	−12.02
II	−4.87	0.37	−11.68	−9.74
III	−4.15	−4.03	−23.69	−21.00
IV	−4.80	−0.65	−18.14	−16.80
V	−4.87	13.98		−32.69

[a] Including ZPE corrections. [b] Including TCE corrections at 298 K.

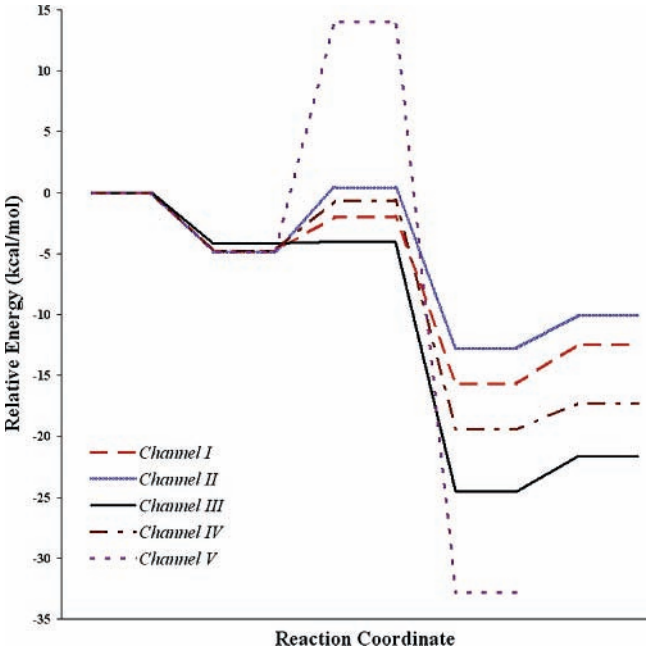

Figure 5. Reaction profiles corresponding to the different channels of IPCP + OH reaction, computed at CCSD(T)//BHandHLYP/6-311++G(d,p).

states corresponding to channels II and V. Therefore, negative overall energy barriers ($E_{overall} = E_{TS} - \Sigma E_{reactants}$) are observed for the hydrogen abstractions channels I, III and IV. According to the reaction profiles (Figure 5), it could be expected channel III to be the main path, because it presents the lowest barrier. On the other hand, the addition channel shows a much higher barrier than any of the abstraction channels, suggesting that this process is very unlikely to occur, and consequently this path was not included in the kinetic calculations. The stabilization energies of the reactant complexes ($E_{RC} - E_{React}$) for all the modeled abstractions are larger than 4 kcal/mol, supporting the complex mechanism assumption.

Intrinsic reaction coordinate calculations (IRC) have been performed at the BHandHLYP/6-311++G(d,p) level of theory to obtain the minimum energy paths (MEP). The calculations were carried out starting from the fully optimized saddle-point geometries, and then moving downhill along the reactant and product channels, in mass-weighted Cartesian coordinates. One hundred points were calculated in each direction at an even gradient step size of 0.01 bohr. The reaction coordinate s is defined as the signed distance from the saddle point, with $s < 0$ referring to the reactants side and $s > 0$ to the products side. As a reasonable compromise between speed and accuracy, twenty points, 10 on each side of the saddle point, were chosen to construct the MEP. Their energies were improved by single point calculations at the CCSD(T)/6-311++G(d,p) level of theory, and they were used in conjunction with gradients and frequencies computed at the BHandHLYP/6-311++G(d,p) level. Figure 6 presents the ground state vibrationally adiabatic

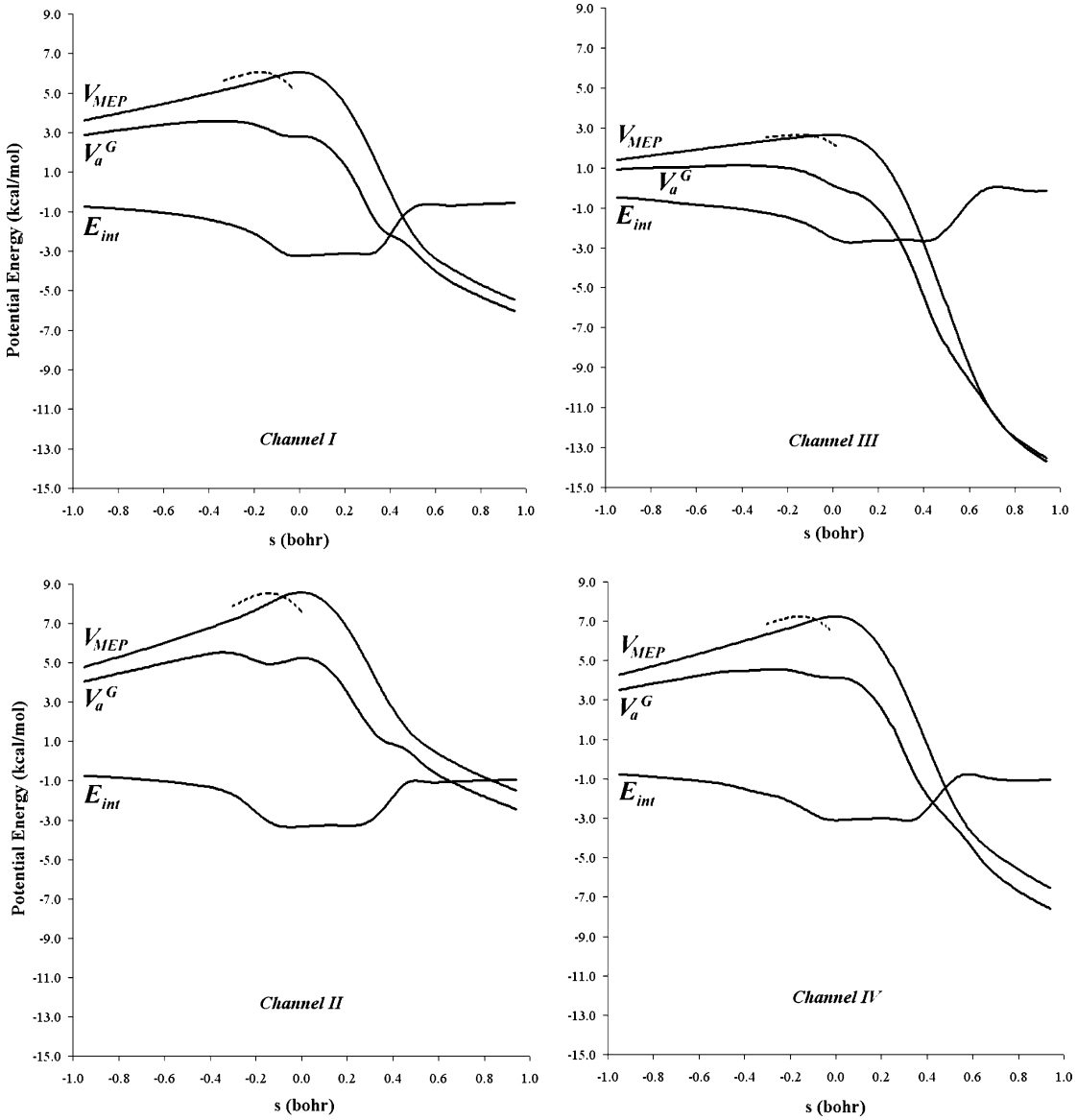

Figure 6. Classical potential energy paths (V_{MEP}) calculated at the CCSD(T) level, internal energies (E_{int}) calculated at the BHandHLYP level, and vibrationally adiabatic potential energy curves (V_a^G) as a function of the reaction coordinate, *s*. All the energies are relative to the corresponding reactant complexes.

potential energy paths for the hydrogen abstractions from IPCP, according to

$$V_a^G(s) = V_{MEP}(s) + E_{int}(s) \quad (6)$$

where $V_{MEP}(s)$ is the classical potential energy path (the CCSD(T) electronic profile) and $E_{int}(s)$ is the local zero-point energy (ZPE) at *s*.

In Figure 6, the electronic curve (V_{MEP}) is represented twice. The dashed line is the electronic energy obtained using the CCSD(T) single point calculations at the BHandHLYP geometries. This procedure for the calculation of the MEP has become common in the study of polyatomic systems because it is relatively inexpensive from a computational point of view and it usually reproduces correctly the main features of the reaction path. It is known as B//A, and it consists of geometry optimizations at a given level (A) followed by single point calculations, without optimization, at a higher level (B). The V_{MEP} obtained using this technique presents a maximum that is shifted toward the reactants valley by about −0.2 bohr with respect to the maximum at the A level of calculation. Espinosa-Garcia and Corchado[59] argue that, when the MEP is constructed using the B//A technique, the energy maximum is artificially located away from the saddle point corresponding to the level of optimization (A). This shift, which is simply a numerical effect, could be mistaken with a variational effect and mislead the kinetic calculations. Consequently, we have used the modification proposed by Espinosa-Garcia and Corchado,[59] which consists of simply moving the maximum of the single-point calculation curve, B//A, to its original position ($s = 0$) at the A//A level. The corresponding curves for V_{MEP} are shown as solid lines in Figure 6. It should be noticed that according to this procedure the frequencies are not shifted; i.e., to each geometry at the A//A level there corresponds a set of original frequencies (calculated at the A//A level) and a shifted energy (calculated at the B//A level).

The potential energy curves for all the abstraction channels of the OH + IPCP reaction are very similar. However, the surface corresponding to channel III is significantly flatter than the others. The behavior of V_a^G and E_{int} is also quite similar in

shape to the one for a methyl hydrogen abstraction reaction by the Cl radical recently studied by Rosenman et al.[60] and to those of glyoxal,[61] methylglyoxal[61] and glycolaldehyde[62] + OH reactions. Because V_a^G is obtained by summing V_{MEP} and E_{int}, the substantial drop in the E_{int} curve prior to the saddle point zone is responsible for the shape of the overall ground-state vibrationally adiabatic surface (V_a^G). The drop in the zero point energy, E_{int}, is not unique and it is characteristic of hydrogen abstraction reactions. Some examples can be found in refs 60−65. When this kind of profile is combined with a low and broad classical barrier, such as the one corresponding to channel III, it causes a large shift of the variational transition state; i.e., there is a large variational effect (see ref 60 for more details). In these cases, the recrossing problem is essential, and variational transition state theory (VTST) theory is needed to obtain reliable values of the rate constants.

Rate Coefficients. According to the reaction mechanism proposed above, if k_1 and k_{-1} are the forward and reverse rate constants for the first step and k_2 corresponds to the second step, a steady-state analysis leads to a rate coefficient for the overall reaction channel that can be written as

$$k = \frac{k_1 k_2}{k_{-1} + k_2} \tag{7}$$

Even though the energy barrier for k_{-1} is about the same size as that for k_2, the entropy change is much larger in the reverse reaction than in the formation of the products. Thus, k_{-1} is expected to be considerably larger than k_2. On the basis of this assumption, first considered by Singleton and Cvetanovic,[66] k can be rewritten as

$$k = \frac{k_1 k_2}{k_{-1} + k_2} = K_{eq} k_2 \tag{8}$$

where K_{eq} is the equilibrium constant between the isolated reactants and the reactant complex and k_2 is the rate constant corresponding to the second step of the mechanism, i.e., transformation of the reactant complex into products. We have assumed that the reactant complex undergoes collisional stabilization; that is, the reaction occurs at the high pressure limit. We have used this limit as our working hypothesis, because there is no experimental evidence that indicates otherwise. This approach has been successfully used to describe OH radical reactions with several volatile organic compounds (VOCs).[61,62,67−71] In a classical treatment the influence of the complex exactly cancels in eq 8 and the overall rate coefficient depends only on properties of OH, IPCP and the transition states. However, in the present case, there is a possibility of quantum mechanical tunneling, and the existence of the complex means that there are extra energy levels from where tunneling may occur so that the tunneling factor, κ, increases. We have assumed that a thermal equilibrium distribution of energy levels is maintained, which corresponds to the high-pressure limiting behavior. Thus, energy levels from the bottom of the well of the complex up to the barrier might contribute to tunneling.

The shape of the MEPs suggests that CVT must be used to study the abstraction channels of the IPCP + OH reaction. Tunneling corrections have been computed using the SCT method. According to eq 2, the CVT, like every TST approach, includes the reaction path symmetry factor, $\sigma(s)$, which accounts for the number of equivalent reaction paths. In this work it was calculated according to the general expression[72−75]

$$\sigma(s) = \frac{n\sigma^R}{\sigma^{GT}(s)} \tag{9}$$

where n is the number of identical transition states, σ^R is the product of the usual rotational symmetry numbers of both reactants, and $\sigma^{GT}(s)$ is the usual symmetry number for the generalized transition state at s. In this work, as usual, σ^{GT} was considered independent of s, thus $\sigma(s)$ becomes a constant σ.

It has been assumed that neither mixing nor crossover between different pathways occurs. Thus, the overall rate constant ($k_{overall}$) has been determined as the sum of the rate coefficients of each path.[76]

Because accurate rate constant calculations require the proper computation of the partition functions (Q), the hindered rotor approximation has been used to correct the Q's corresponding to internal rotations with torsional barriers comparable to RT. Direct inspection of the low-frequency modes of the studied stationary points indicates that there are several modes that correspond to hindered rotations. These modes should be treated as hindered rotors instead as vibrations.[77] To make this correction, these modes were removed from the vibrational partition function of the corresponding speciesand replaced with the hindered rotor partition function (Q^{HR}).

The overall rate coefficients calculated in the 260−350 K temperature range are reported in Table 3, together with the branching ratios (Γ) corresponding to the different abstraction channels (Γ). They have been calculated as

$$\Gamma_{I,II,IIIorIV} = \frac{k_{I,II,IIIorIV}}{k_{overall}} \times 100 \tag{10}$$

The very good agreement between the experimental and calculated values of $k_{overall}$, at 298 K support the reliability of the data reported here for the first time. It also supports the validity of the proposed mechanism and of the level of theory used for both electronic and rate constant calculations. According to our results, the abstractions mainly occur through channel III. As the temperature increases, the proportion of H abstraction from sites other than this slightly increases. However, abstraction from the - -CH< group in the isopropyl side remains dominant over the whole range of the studied temperatures. The variational transition states corresponding to paths I, II, III and IV are located on the reactants side, at s values around −0.37, −0.32, −0.38 and −0.27 bohr, respectively, for the whole temperature range. Tunneling effects were found to be small but relevant in all the cases.

The influence of temperature on the rate of the chemical reactions studied in this work has been interpreted in terms of the Arrhenius equation:[78]

$$k = Ae^{--E_a/RT} \tag{11}$$

where A is known as the preexponential factor or the frequency factor, and E_a represents the activation energy.

The ln k vs $1/T$ plots corresponding to the four partials and the *overall* rate coefficients were found to be linear, supporting the use of the Arrhenius equation to describe their temperature dependences. Thus, the activation energies do not change in the studied temperature range. Negative temperature dependences were obtained for the overall reaction as well as for channel III. Rate coefficients increase with temperature for all the other channels. The proposed Arrhenius parameters are reported in Table 4.

Conclusions

The OH abstraction reaction from isopropylcyclopropane seems to occur through a complex mechanism involving the

TABLE 3: Rate Coefficients, in cm^3 molecule^{-1} s^{-1}, and Branching Ratios (Γ), within the Temperature Range 260−350 K

T	$10^{12}k_{overall}$	Γ_I	Γ_{II}	Γ_{III}	Γ_{IV}
260	3.63	0.56	0.01	98.40	1.03
270	3.40	0.62	0.01	98.17	1.20
280	3.19	0.69	0.02	97.92	1.38
290	3.02	0.75	0.02	97.66	1.57
292	2.98	0.76	0.02	97.61	1.61
294	2.95	0.78	0.02	97.55	1.65
296	2.92	0.79	0.03	97.50	1.69
298.15	**2.89**	**0.80**	**0.03**	**97.44**	**1.73**
300	2.86	0.81	0.03	97.39	1.77
302	2.83	0.83	0.03	97.33	1.81
304	2.81	0.84	0.03	97.27	1.85
306	2.78	0.85	0.03	97.22	1.90
308	2.75	0.87	0.03	97.16	1.94
310	2.73	0.88	0.04	97.10	1.99
320	2.61	0.94	0.04	96.80	2.21
330	2.50	1.01	0.05	96.50	2.44
340	2.40	1.07	0.07	96.18	2.68
350	2.32	1.13	0.08	95.86	2.93

TABLE 4: Arrhenius Parameters in the 260−350 K Temperature Range

	$10^{13}A^a$	$E_a{}^b$
$k_{overall}$	6.77	−0.86
k_I	0.54	0.51
k_{II}	2.88	3.51
k_{III}	6.05	−0.91
k_{IV}	3.84	1.21

[a] cm^3 molecule^{-1} s^{-1}. [b] kcal/mol.

formation of a reactant complex in the entrance channel and of a product complex in the exit channel, for each abstraction path. The addition of OH to the cyclopropyl ring does not contribute to the overall reaction. The unexpected reactant complexes are caused by interactions between the H atom in the OH radical and the cyclopropyl ring in the IPCP, in an alkene-like kind of interaction.

The MEP was computed using the two-level theory approach known as B//A, which consists of a geometry optimization at level A, followed by a single point calculation at a higher level B. The chosen levels were A = BHandHLYP/6-311++G(d,p) and B = CCSD(T)/6-311++G(d,p). The vibrationally adiabatic potential energy surfaces were found to be low and broad, supporting the use of the CVT/SCT approach to calculate the rate coefficients.

The abstraction from the −CH< site in the isopropyl group was found to be dominant within the whole temperature range, varying from 98% at 260 K to 96% at 350 K. At 298 K its contribution to the overall reaction was found to be 97.4%. The calculated overall rate coefficient ($k_{overall}$) was found to be equal to 2.89×10^{-12} cm^3 molecule^{-1} s^{-1}, in excellent agreement with the experimental value previously reported.

The temperature dependence of the overall rate coefficient is best fitted by the Arrhenius expression $k_{overall} = 6.67 \times 10^{-13}e^{434/RT}$ cm^3 molecule^{-1} s^{-1}. The predicted activation energy is −0.86 kcal/mol, in the 260−350 K temperature range.

Acknowledgment. We gratefully acknowledge the financial support from the Instituto Mexicano del Petróleo (IMP) through projects D00237 and D00345 as well as from the "Programa de Apoyo a la Investigacion y Posgrado de la Facultad de Química de la UNAM". We also thank the IMP Computing Center for supercomputer time on SGI Origin 3000. We thank professors S. Zhang and T. N. Truong for providing access to the cseo.net site through Internet.[20]

References and Notes

(1) Atkinson, R.; Aschmann, S. M. *Int. J. Chem. Kinet*. **1988**, *20*, 339.
(2) Atkinson, R. *Atmos. Chem. Phys. Discuss*. **2003**, *3*, 4183.
(3) Atkinson, R. *Chem. Rev*. **1986**, *86*, 69.
(4) Atkinson, R. *Int. J. Chem. Kinet*. **1986**, *18*, 555.
(5) Atkinson, R. *Int. J. Chem. Kinet*. **1987**, *19*, 799.
(6) Kwok, E. S. C.; Atkinson, R. *Atmos. Env*. **1995**, *29*, 1685.
(7) Frisch, M. J.; Trucks, G. W.; Schlegel, H. B.; Scuseria, G. E.; Robb, M. A.; Cheeseman, J. R.; Zakrzewski, V. G.; Montgomery Jr., J. A.; Stratmann, R. E.; Burant J. C.; Dapprich, S.; Millam, J. M.; Daniels, A. D.; Kudin, K. N.; Strain, M. C.; Farkas, O.; Tomasi, J.; Barone, V.; Cossi, M.; Cammi, R.; Mennucci, B.; Pomelli, C.; Adamo, C.; Clifford, S.; Ochterski, J.; Petersson, G. A.; Ayala, P. Y.; Cui, Q.; Morokuma, K.; Malick, D. K.; Rabuck, A. D.; Raghavachari, K.; Foresman, J. B.; Cioslowski, J.; Ortiz, J. V.; Stefanov, B. B.; Liu, G.; Liashenko, A.; Piskorz, P.; Komaromi, I.; Gomperts, R.; Martin, R. L.; Fox, D. J.; Keith, T.; Al-Laham, M. A.; Peng, C. Y.; Nanayakkara, A.; Gonzalez, C.; Challacombe, M.; Gill, P. M. W.; Johnson, B.; Chen, W.; Wong, M. W.; Andres, J. L.; Gonzalez, C.; Head-Gordon, M.; Replogle, E. S.; Pople, J. A. *Gaussian 98*, revision A.3; Gaussian Inc.: Pittsburgh, PA, 1998.
(8) Becke, A. D. *J. Chem. Phys*. **1993**, *98*, 1372.
(9) Raghavachari, K.; Foresman, J. B.; Cioslowski, J.; Ortiz, J. V.; Frisch, M. J.; Frisch, A. *GAUSSIAN* 98 *User's Reference*; Gaussian Inc.: Pittsburgh, PA, 1998.
(10) Keck, J. C. *J. Chem. Phys*. **1960**, *32*, 1035.
(11) Baldridge, K. M.; Gordon, M. S.; Steckler, R.; Truhlar, D. G. *J. Phys. Chem*. **1989**, *93*, 5107.
(12) Garrett, B. C.; Truhlar, D. G.; Grev, R. S.; Magnuson, A. W. *J. Phys. Chem*. **1980**, *84*, 1730; Erratum. *J. Phys. Chem*. **1983**, *87*, 4554.
(13) Isaacson, A. D.; Truhlar, D. G. *J. Chem. Phys*. **1982**, *76*, 1380.
(14) Truhlar, D. G.; Isaacson, A. D.; Garrett, B. C. *Theory of Chemical Reaction Dynamics*; Baer, M., Ed.; CRC Press: Boca Raton, FL, 1985; Vol. 4, pp 65−137.
(15) Truhlar, D. G.; Garrett, B. C. *Annu. Rev. Phys. Chem*. **1984**, *35*, 159.
(16) Lu, D.-h.; Truong, T. N.; Melissas, V.; Lynch, G. C.; Liu, Y.-P.; Garrett, B. C.; Steckler, R.; Isaacson, A. D.; Rai, S. N.; Hancock, G. C.; Lauderdale, J. G.; Joseph, T.; Truhlar, D. G. *Comput. Phys. Commun*. **1992**, *71*, 235.
(17) Truhlar, D. G.; Gordon, M. S. *Science* **1990**, *249*, 491.
(18) Truong, T. N.; Lu, D.-h.; Lynch, G. C.; Liu, Y.-P.; Melissas, V. S.; Stewart, J. J. P.; Steckler, R.; Garrett, B. C.; Isaacson, A. D.; Gonzalez-Lafont, A.; Rai, S. N.; Hancock, G. C.; Joseph, T.; Truhlar, D. G. *Comput. Phys. Commun*. **1993**, *75*, 143.
(19) Liu, Y.-P.; Lynch, G. C.; Truong, T. N.; Lu, D.-h.; Truhlar, D. G.; Garrett, B. C. *J. Am. Chem. Phys*. **1993**, *115*, 2408.
(20) Zhang, S.; Truong, T. N. *Kinetics* (CSEO version 1.0); University of Utah: Salt Lake City, 2003.
(21) Truhlar, D. G.; Kupperman, A. *J. Am. Chem. Soc*. **1971**, *93*, 1840.
(22) Fukui, K. *Pure Appl. Chem*. **1982**, *54*, 1825.
(23) Fukui, K. *J. Phys. Chem*. **1970**, *74*, 4161.
(24) Gonzalez, C.; Schlegel, H. B. *J. Phys. Chem*. **1990**, *94*, 5523.
(25) Truhlar, D. G. Kupperman, A. *J. Am. Chem. Soc*. **1971**, *93*, 1840.
(26) Truhlar, D. G.; Isaacson, A. D.; Garrett, B. C. In *Theory of Chemical Reaction Dynamics*; Baer, M., Ed.; CRC Press: Boca Raton, FL, 1985; Vol. 4, p 65.
(27) Eyring, H. *J. Chem. Phys*. **1935**, *3*, 107.
(28) Truhlar, D. G.; Hase, W. L.; Hynes, J. T. *J. Phys. Chem*. **1983**, *87*, 2664.
(29) Truhlar, D. G.; Garrett, B. C. *Acc. Chem. Res*. **1980**, *13*, 440.
(30) Truhlar, D. G.; Garrett, B. C. *Annu. Rev. Phys. Chem*. **1984**, *35*, 159.
(31) Truhlar, D. G.; Isaacson, A. D.; Garrett, B. C. In *Generalized transition state theory*; Truhlar, D. G., Isaacson, A. D., Garrett, B. C., Eds.; CRC Press: Boca Raton, FL, 1985; Vol. 4, p 65.
(32) Garrett, B. C.; Truhlar; D. G. *J. Phys. Chem*. **1979**, *83*, 1052.
(33) Garrett, B. C.; Truhlar; D. G. *J. Phys. Chem*. **1979**, *83*, 1079.
(34) Garrett, B. C.; Truhlar; D. G. *J. Am. Chem. Soc*. **1979**, *101*, 4534.
(35) Garrett, B. C.; Truhlar; D. G. *J. Phys. Chem*. **1979**. *83* 3058.
(36) Schenter, G. K.; Garrett, B. C.; Truhlar, D. G. *J. Chem. Phys*. **2003**, *119*, 5828.
(37) Ayala, P. Y.; Schlegel, H. B. *J. Chem. Phys*. **1998**, *108*, 2314.
(38) Marcus, R. A.; Coltrin, M. E. *J. Chem. Phys*. **1977**, *67*, 2609.
(39) Lu, D.-h.; Truong, T. N.; Melissas, V. S.; Lynch, G. C.; Liu, Y.-P.; Garrett, B. C.; Steckler, R.; Isaacson, A. D.; Rai, S. N.; Hancock, G. C.; Lauderdale, J. G.; Joseph, T.; Truhlar, D. G. *Comput. Phys. Commun*. **1992**, *71*, 235.
(40) Liu, Y.-P.; Lynch, G. C.; Truong, T. N.; Lu, D.-h.; Truhlar, D. G.; Garrett, B. C. *J. Am. Chem. Soc*. **1993**, *115*, 2408.
(41) Díaz-Acosta, I.; Alvarez-Idaboy, J. R.; Vivier-Bunge, A. *Int. J. Chem. Kinet*. **1999**, *31*, 29.
(42) Coulson, C. A.; Moffitt, W. E. *Philos. Mag*. **1949**, *40*, 1.

(43) Weigert, F. J.; Roberts, J. D. *J. Am. Chem. Soc*. **1967**, *89*, 5692.
(44) Hay, P. J.; Hunt, W. J.; Goddard, W. A., III. *J. Am. Chem. Soc*. **1972**, *94*, 8293.
(45) Maksie, Z. B.; Randie, M. *J. Am. Chem. Soc*. **1973**, *95*, 6522.
(46) Allen, F. H. *Acta Crystallogr*. **1981**, *B37*, 890.
(47) Karadakov, P. B.; Gerratt, J.; Cooper, D. L.; Raimondi, M. *J. Am. Chem. Soc*. **1994**, *116*, 7714.
(48) Sproviero, E. M.; Ferrara, A.; Contreras, R. H.; Burton, G. J. *Chem. Soc., Perkin Trans. 2* **1996**, 933.
(49) Sproviero, E. M.; Burton, G. *J. Phys. Chem. A* **2002**, *106*, 7834.
(50) Foster, J. P.; Weinhold, F. *J. Am. Chem. Soc*. **1980**, *102*, 7211.
(51) Reed, A. E.; Weinhold, F. *J. Chem. Phys.* **1983**, *78*, 4066.
(52) Reed, A. E.; Weinhold, F. *J. Chem. Phys*. **1983**, *78*, 1736.
(53) Reed, A. E.; Weinstock, R. B.; Weinhold, F. *J. Chem. Phys*. **1985**, *83*, 735.
(54) Reed, A. E.; Curtiss, L. A.; Weinhold, F. *Chem. Rev.* **1988**, *88*, 899.
(55) Glendening, E. D.; Reed, A. E.; Carpenter, J. E.; Weinhold, F.; NBO Version 3.1.
(56) Pauling, L., *J. Am. Chem. Soc*. **1931**, *53*, 1367.
(57) Slater, J., *C. Phys. Rev*. **1931**, *37*, 481.
(58) Bader, R. F. W. *Atoms in Molecules—A Quantum Theory*; Oxford University Press: Oxford, NY, 1990.
(59) Espinosa-Garcia, J.; Corchado, J. C. *J. Phys. Chem.* **1995**, *99*, 8613.
(60) Rosenman, E.; McKee, M. L. *J. Am. Chem. Soc*. **1997**, *119*, 9033.
(61) Galano, A.; Alvarez-Idaboy, J. R.; Ruiz-Santoyo, M. E.; Vivier-Bunge, A. *Chem. Phys. Chem*. **2004**, *5*, 1379.
(62) Galano, A.; Alvarez-Idaboy, J. R.; Ruiz-Santoyo, Ma. E.; Vivier-Bunge, A. *J. Phys. Chem. A* **2004**, *109*, 169.
(63) Corchado, J. C.; Espinosa-Garcia, J. *J. Chem. Phys.* **1997**, *106*, 4013.
(64) Natanson, G. A. *Chem. Phys. Lett.* **1992**, *190*, 209.
(65) Espinosa-Garcia, J.; Corchado, J. C. *J. Chem. Phys.* **1994**, *101*, 1333.
(66) Singleton, D. L.; Cvetanovic, R. J. *J. Am. Chem. Soc*. **1976**, *98*, 6812.
(67) Alvarez-Idaboy, J. R.; Mora-Diez, N.; Vivier-Bunge, A. *J. Am. Chem. Soc.* **2000**, *122*, 3715.
(68) Alvarez-Idaboy, J. R.; Mora-Diez, N.; Boyd, R. J.; Vivier-Bunge, A. *J. Am. Chem. Soc*. **2001**, *123*, 2018.
(69) Galano, A.; Alvarez-Idaboy, J. R.; Bravo-Perez, G.; Ruiz-Santoyo, M. E.; *Phys. Chem. Chem. Phys*. **2002**, *4*, 4648.
(70) Galano, A.; Alvarez-Idaboy, J. R.; Ruiz-Santoyo, M. E.; Vivier-Bunge, A. *J. Phys. Chem. A* **2002**, *106*, 9520.
(71) Alvarez-Idaboy, J. R.; Cruz-Torres, A.; Galano, A.; Ruiz-Santoyo, M. E. *J. Phys. Chem. A* **2004**, *108*, 2740.
(72) Pechukas, P. *J. Chem. Phys*. **1976**, *64*, 1516.
(73) Pechukas, P. *Dinamics of Molecular Collision*; Miller, W. H., Ed.; Plenum Press: New York, 1976; Part B.
(74) Pollak, E.; Pechukas, P. *J. Am. Chem. Soc*. **1978**, *100*, 2984.
(75) Gilbert, R. G.; Smith, S. C. *Theory of Unimolecular and Recombination Reactions*; Blackwell Scientific Publications: Oxford, U.K., 1990.
(76) Robinson, P. J.; Holbrook, K. A.; *Unimolecular Reactions*; Wiley-Interscience: London, 1972.
(77) Jacox, M. E. *Vibrational and Electronic Energy Levels of Polyatomic Transient Molecules*; NIST: Gaithersburg, MD, 1998; Vol. 69, p 945.
(78) Arrhenius, S. *Z. Phys. Chem.* **1889**, *4*, 226.